

Effect of Chloride Ion on Corrosion of Mild Steel in the 7.0 mol/L H₃PO₄ Solution in the Presence of 1,10-Phenanthroline

Ji-Tong Gong, Yi-Jing Liu, Lin Wang*, Yan Qin, Yin-long Bai, Dong-Mei Lu

School of Chemical Science and Technology, Key Laboratory of Medicinal Chemistry for Nature Resource, Ministry of Education, Yunnan University, Kunming, Yunnan, 650091, P. R. China

*E-mail: wanglin@ynu.edu.cn (L. Wang); wanglin2812@163.com

Received: 4 February 2020 / Accepted: 7 April 2020 / Published: 10 May 2020

The inhibition effects of chloride ion and 1,10-phenanthroline (PTL) on the corrosion of mild steel in 7.0 mol/L H₃PO₄ solution were studied by potentiodynamic polarization, electrochemical impedance spectroscopy and weight loss techniques. The results reveal that Cl⁻ can inhibit the corrosion of mild steel in 7.0 mol/L H₃PO₄ solution to some extent, while the combination of Cl⁻ and PTL obviously improves the corrosion inhibition and shows better synergistic inhibition effect on mild steel corrosion in 7.0 mol/L H₃PO₄ solution. The electrochemical studies indicate that Cl⁻ alone or the combination of Cl⁻ and PTL acts as a mixed type of inhibitor for mild steel in 7.0 mol/L phosphoric acid and the corrosion reaction is controlled by charge transfer. The adsorption of Cl⁻ on the mild steel surface follows Langmuir adsorption isotherm in the absence or presence of PTL. The kinetic and thermodynamic parameters (E_a , ΔH_a , ΔS_a , K_{ads} and ΔG°_{ads}) were calculated and discussed. The adsorption process of the inhibitor molecules on the mild steel surface is spontaneous and contains coexistence of physical and chemical adsorption, while physical adsorption is absolutely dominant.

Keywords: Corrosion, 1,10-Phenanthroline, Chloride ion, Mild steel, Phosphoric acid, Synergistic inhibition.

1. INTRODUCTION

Phosphoric acid, as a moderately strong acid, also shows relatively strong corrosion effect on steel [1-3]. In general, the researches on the corrosion inhibition of steel in phosphoric acid solution are relatively fewer, and these studies are also mainly carried out in lower concentration phosphoric acid solution [4-16]. In phosphoric acid industry, the concentration of phosphoric acid involved is relatively high. The concentration of phosphoric acid produced is about 4~5.5 mol/L H₃PO₄ (30%~40% H₃PO₄) for the dihydrate wet-method process, and for the hemihydrate wet-method process, the concentration of phosphoric acid is approximately 7.5~9 mol/L H₃PO₄ (55%~63% H₃PO₄)

[17]. The corrosion of metallic material equipment cannot be ignored in the production of phosphorus chemical industry. Physical protection is mainly adopted in the phosphoric acid industry, such as the use of protective lining tiles, steel lining rubber to extend the service life of production equipment, and a few core equipment are even made of high-grade stainless [17]. These protective tiles and lining rubber also need to be replaced with new ones after a certain period of use. Even high-grade stainless steel will be gradually eroded in use. It is an economical, convenient and effective way to apply corrosion inhibitor to metal corrosion protection [18-19]. Many effective inhibitors are organic compounds containing N, S, O heteroatoms, π -electrons and conjugated structures [20-29].

Phosphate rock contains chloride impurities. These chlorides will be brought into the production process. Chloride ion is harmful to stainless steel equipment to a certain extent [17, 30]. Stainless steel will suffer pitting corrosion under the influence of chloride ion [31]. However, some studies also show that chloride ion has a certain inhibition effect on mild steel in acid solution, and it has a good synergistic inhibition with some inhibitors [32-35]. Mild steel is one of the most important metals and widely used as constructional material in many industries because it is low cost and excellent mechanical properties [36].

As an indicator in analytical chemistry, 1,10-phenanthroline (PTL) contains abundant π -electrons heterocyclic and nitrogen atoms unshared electron pairs, which could transfer the unshared electron pairs to the d -orbitals of iron surface atoms. This nitrogen-containing heterocyclic compound should meet the requirements as an inhibitor for the corrosion of steel in acid solution. In the present work, the corrosion of mild steel in the 7.0 mol/L H_3PO_4 solution in the presence of chloride ion without and with 1,10-phenanthroline has been researched by potentiodynamic polarization, electrochemical impedance spectroscopy (EIS) and weight loss techniques.

2. EXPERIMENTAL

2.1. Materials

The mild steel specimens have a chemical composition of (wt%): 0.10% C, 0.026% P, 0.017% S, 0.28% Mn, 0.05% Si and Fe balance.

Bidistilled water was used to prepare the experimental solutions and AR grade H_3PO_4 and potassium chloride were used too. 1,10-Phenanthroline (99%) was supplied by Merck Chemicals. Figure 1. gives the chemical structure of PTL.

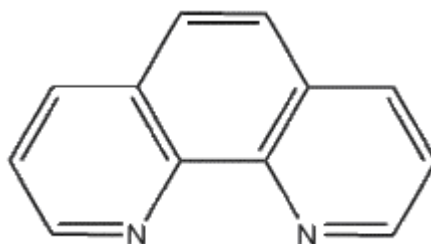


Figure 1. Structure of 1,10-Phenanthroline.

2.2. Electrochemical measurements

The electrochemical measurements were conducted in a conventional three-electrode cell. The reference electrode and auxiliary electrode were a saturated calomel electrode (SCE) and platinum foil, respectively. The working electrodes were embedded in PVC holder using epoxy resin with an exposed area of 1.0 cm². Each working electrode was polished using emery papers from 300 to 1200 grades on the test face, washed with distilled water, degreased with acetone, and dried with a warm air stream. Before each measurement, the working electrode was immersed in the 250 mL testing solution for two hours at open circuit potential (OCP) until corrosion potential reached a steady state.

All the electrochemical experiments were carried out by PARSTAT 2263 Potentiostat/Galvanostat (Princeton Applied Research). The potentiodynamic polarization curves were obtained by changing the electrode potential from -250mV to + 250mV versus the open circuit potential, at a sweeping rate of 0.5 mVs⁻¹. EIS experiments were performed in the frequency range of 10 mHz to 100 kHz using a 10 mV peak to peak voltage excitation. Each experiment was performed in triplicate to ensure reproducibility at 30°C.

2.3. Weight loss measurements

The specimens (40 mm × 15 mm × 0.4 mm) were successively polished with emery papers (300 - 1200 grade), washed in distilled water, degreased in acetone and dried in a stream of air.

The specimens were weighed accurately before immersion in testing solutions (150 mL) for four hours in air without bubbling. At the end of the run the specimens were taken out, washed with distilled water then acetone, dried and immediately weighed. The weight loss tests were completed at 20, 30, 40 and 50°C respectively. Each measurement was performed on three separate samples and the average weight loss was taken.

3. RESULTS AND DISCUSSION

3.1. Polarization measurements

The potentiodynamic polarization curves of mild steel for different concentrations of chloride ion in the absence and presence of 0.5 mmol/L PTL in 7.0 mol/L H₃PO₄ at 30°C are given in Figure 2 and Figure 3, respectively.

From Figure 2, chloride ion slightly changed the corrosion potential to both negative and positive directions and caused a decrease of current density of anode or cathode, however, it is clear that the anode polarization was dominant. These showed that chloride ion has a certain inhibition effect on the cathodic hydrogen evolution reaction and the dissolution of anode metal, which means that chloride ion is a mixed-type inhibitor for mild steel corrosion in 7.0 mol/L H₃PO₄ solution. Figure 3 compared with figure 2, with the addition of 0.5 mmol/L PTL, it is obvious that the shifting levels of anodic and cathodic in the presence PTL is much greater than those in the absence of PTL, and

combination of chloride ion and PTL also slightly shifted E_{corr} to negative and positive directions. These results also showed that combination of chloride ion and PTL is still a mixed-type inhibitor for mild steel corrosion in 7.0 mol/L H_3PO_4 solution.

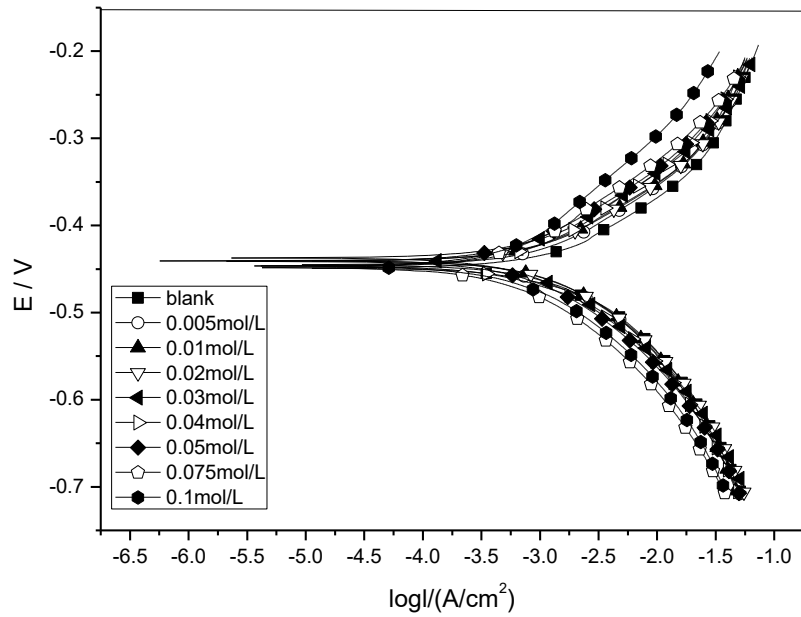


Figure 2. Potentiodynamic polarization curves of mild steel containing different concentrations of Cl^- in the 7.0 mol/L H_3PO_4 at 30°C.

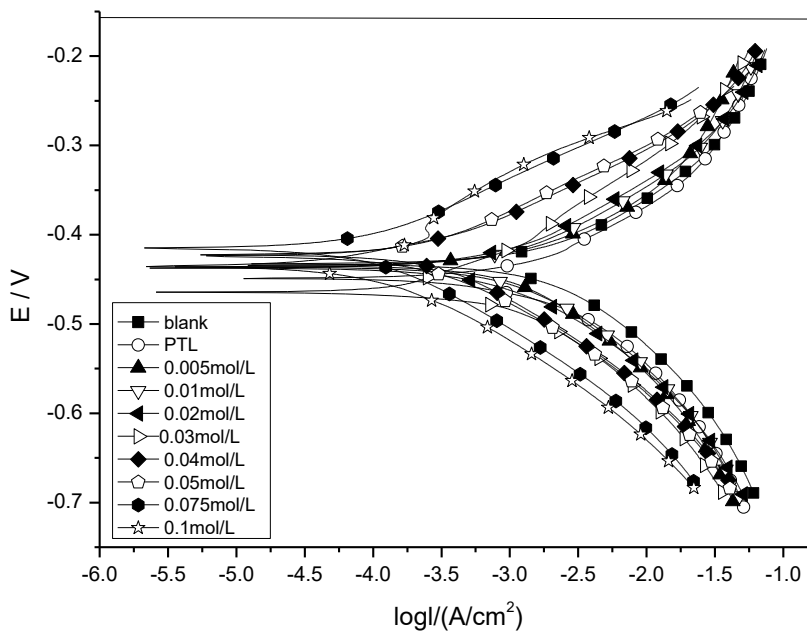


Figure 3. Potentiodynamic polarization curves of mild steel containing different concentrations of Cl^- with 0.5 mmol/L PTL in the 7.0 mol/L H_3PO_4 at 30°C.

A few studies have also indicated that chloride ion, as a mixed-type inhibitor, shown a certain inhibition effect on the corrosion of cold rolled steel in low concentration phosphoric acid solution (1.0 mol/L), and has a good synergistic inhibition effect with 4-(2-pyridylazo) resorcin or methyl violet [5,14].

The inhibition efficiency (IE_i) can be obtained by the following formula [37]

$$IE_i = \frac{I_{corr}^0 - I_{corr}^{inh}}{I_{corr}^0} \times 100 \quad (1)$$

where I_{corr}^0 and I_{corr}^{inh} are the corrosion current density values without and with inhibitors, respectively.

Table 1 gives the electrochemical polarization parameters for the mild steel corrosion in 7.0 mol/L H_3PO_4 solution. As can be seen from the Table 1, there is no regular change of the slopes (β_a and β_c) by changing the inhibitor concentrations, which means that the corrosion reaction mechanisms of cathodic hydrogen evolution and anodic steel dissolution did not changed [38-39]. It appears that corrosion inhibition occurred by a blocking mechanism on the reaction active centers of steel surface [40].

Table 1. Electrochemical polarization parameters for mild steel in 7.0 mol/L H_3PO_4 containing different concentrations of Cl^- without and with 0.5 mmol/L PTL at 30 °C.

KCl (mol/L)	PTL (mmol/L)	E_{corr} (vs. SCE) (mV)	I_{corr} ($\mu A/cm^2$)	β_a (mV/dec)	$-\beta_c$ (mV/dec)	IE_i
0	0	-448	2263	43	301	—
0.005	0	-449	1440	44	315	36.3
0.01	0	-441	1416	44	324	37.4
0.02	0	-440	1244	47	320	45.0
0.03	0	-437	1080	46	336	52.3
0.04	0	-449	1048	46	328	53.7
0.05	0	-440	942.3	51	347	58.4
0.075	0	-452	721.2	50	366	68.1
0.1	0	-448	695.7	54	360	70.6
0	0.5	-451	1554	65	556	34.2
0.005	0.5	-432	1152	58	565	49.1
0.01	0.5	-432	928.3	55	610	59.0
0.02	0.5	-439	800.0	56	630	64.7
0.03	0.5	-467	642.5	59	619	71.8
0.04	0.5	-431	480.0	40	603	78.8
0.05	0.5	-432	444.6	41	613	80.4
0.075	0.5	-419	184.2	41	654	91.9
0.1	0.5	-432	165.7	45	681	92.7

Comparing values of I_{corr} and IE_i in the presence of PTL with those in the absence of PTL, it can be seen that the corrosion current density decreased and the inhibition efficiencies improved

effectively, which means the combination of Cl^- and PTL has a better inhibition effect on the corrosion of mild steel in 7.0 mol/L H_3PO_4 solution.

3.2. Electrochemical impedance spectroscopy

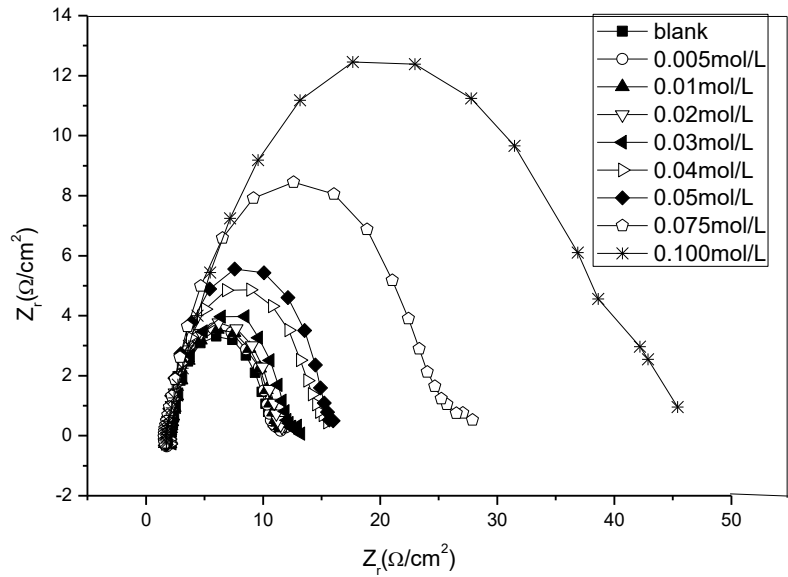


Figure 4. Nyquist plots of the mild steel containing different concentrations of Cl^- in the 7.0 mol/L H_3PO_4 at 30°C.

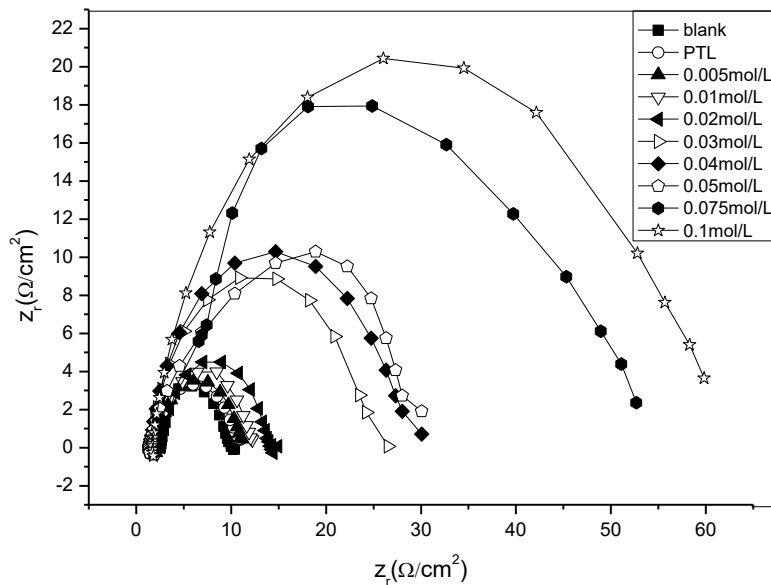


Figure 5. Nyquist plots of the mild steel containing different concentrations of Cl^- with 0.5 mmol/L PTL in the 7.0 mol/L H_3PO_4 at 30°C.

Nyquist plots of mild steel in 7.0 mol/L H₃PO₄ solution for Cl⁻ as inhibitor without and with 0.5 mmol/L PTL are shown in Figure 4 and Figure 5 at 30°C, respectively.

It can be observed that all impedance spectra show a single depressed capacitive loop with and without inhibitors for mild steel in 7.0 mol/L H₃PO₄ solution, indicating that the corrosion process of mild steel occurred mainly under charge transfer control and the presence of inhibitor did not change the mechanism of mild steel dissolution [41]. The capacitive loops are not perfect semicircles because of the frequency dispersion as a result of the roughness and inhomogeneous of electrode surface [42]. The semicircle diameter increased with the increase of Cl⁻ concentration, but it is clear that the radius increased more obviously with the addition of 0.5 mmol/L PTL, indicating that the protection barrier become more thickly packed over the surface of steel and the existence of PTL effectively improved the corrosion inhibition performance of Cl⁻.

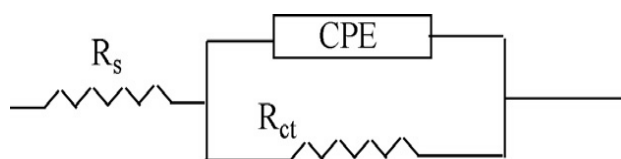


Figure 6. EIS spectra of the inhibitors using the equivalent circuit.

The impedance results of mild steel in 7.0 mol/L H₃PO₄ are analyzed according to the equivalent circuit model, given in Figure 6, which includes charge transfer resistance (R_{ct}), solution resistance (R_s) and constant phase element (CPE). The double layer capacitance (C_{dl}) value affected by imperfections of the surface is simulated via CPE [43]. The CPE is composed of a component Q_{dl} and a coefficient α which quantifies different physical phenomena including surface inhomogeneous resulting from inhibitor adsorption, porous layer formation, surface roughness, etc. The C_{dl} can be calculated from the formula [44]:

$$C_{dl} = Q_{dl} \cdot (2\pi f_{max})^{b-1} \quad (2)$$

where f_{max} represents the frequency at which the imaginary value reaches a maximum on the Nyquist plot.

The inhibition efficiencies (IE_{ct}) could be obtained by the equation:

$$IE_{ct} = \frac{R_{ct}^{inh} - R_{ct}^0}{R_{ct}^{inh}} \times 100 \quad (3)$$

where R_{ct}^0 and R_{ct}^{inh} are the values of the charge-transfer resistances in the absence and presence of inhibitor, respectively. The values of R_{ct} , R_s , C_{dl} , and IE_{ct} are listed in Table 2.

From the Table 2, the values of C_{dl} decrease in the presence of inhibitors compare to the absence of inhibitor, implying that the adsorption of the inhibitors on the steel surface formed an adherent film and increased the thickness of the electrical double layer, which may be responsible for the decrease of C_{dl} [45-46]. The values of R_{ct} and IE_{ct} both increase with increase of Cl⁻ concentration without and with PTL and the increase of R_{ct} or IE_{ct} is obviously larger with than without PTL.

Table 2. EIS parameters for mild steel in 7.0 mol/L H₃PO₄ containing different concentrations of Cl⁻ without and with 0.5 mmol/L PTL at 30 °C.

KI (mmol/L)	MV (mmol/L)	R _s (Ω cm ²)	C _{dl} (μF/cm ²)	R _{ct} (Ω cm ²)	IE _{ct}
0	0	1.58	479	8.79	
0.005	0	1.87	429	10.4	15.5
0.01	0	1.99	401	11.0	20.1
0.02	0	1.69	387	11.7	24.9
0.03	0	2.13	359	12.7	30.8
0.04	0	2.79	330	14.1	37.7
0.05	0	3.53	295	16.5	46.7
0.075	0	4.69	233	21.1	58.3
0.1	0	3.79	203	27.1	67.6
0	0.5	1.88	430	10.4	15.5
0.005	0.5	2.03	377	12.0	26.8
0.01	0.5	2.37	345	13.0	32.4
0.02	0.5	3.39	319	15.2	42.2
0.03	0.5	4.24	217	24.3	63.8
0.04	0.5	3.59	203	26.0	66.2
0.05	0.5	3.79	204	26.9	67.3
0.075	0.5	4.59	129	49.0	82.1
0.1	0.5	3.97	122	53.2	83.5

3.3. Weight loss measurements

The corrosion inhibition efficiencies (*IE_w*) were also obtained by weight loss method:

$$IE_w = \frac{V_0 - V_i}{V_0} \times 100 \quad (4)$$

where *V₀* and *V_i* are the corrosion rates in the absence and presence of the inhibitors, respectively.

Table 3 gives the corrosion rates and inhibition efficiencies of mild steel in 7.0 mol/L H₃PO₄ containing different concentrations of Cl⁻ without and with 0.5 mmol/L PTL at 30 °C.

Table 3. Corrosion rates and inhibition efficiencies obtained by weight loss for the mild steel in 7.0 mol/L H₃PO₄ containing different concentrations of Cl⁻ without and with 0.5 mmol/L PTL at 30 °C.

Cl ⁻ (mol/L)	PTL (mmol/L)	V (g/m ² h)	IE _w
0	0	43.89	
0.005	0	28.23	35.7
0.01	0	26.15	40.4
0.02	0	23.26	47.0
0.03	0	19.68	55.2

0.04	0	19.01	56.7
0.05	0	16.84	61.6
0.075	0	14.68	66.6
0.1	0	12.43	71.7
0	0.5	29.84	32.0
0.005	0.5	21.91	50.1
0.01	0.5	18.44	58.0
0.02	0.5	15.56	64.5
0.03	0.5	12.87	70.7
0.04	0.5	9.766	77.8
0.05	0.5	8.444	80.8
0.075	0.5	4.828	89.0
0.1	0.5	3.274	92.5

With the increase of Cl^- concentration, the corrosion rate decreased and the inhibition efficiency increased. It is also seen that the IE_w have been greatly improved with the addition of 0.5 mmol/L PTL. These results are in good agreement with those obtained from electrochemistry measurements.

3.4. Effect of temperature

Temperature has an important influence on metal corrosion in acid solution. Table 4 gives the effect of temperature change (30-45 °C) on corrosion rate of mild steel in 7.0 mol/L H_3PO_4 in the absence and presence of 0.05 mol/L Cl^- without and with 0.5 mmol/L PLT by weight loss method.

Table 4. The effect of temperature on the corrosion rates(V) of mild steel in 7.0 mol/L H_3PO_4 in the absence and presence of 0.05 mol/L Cl^- without and with 0.5 mmol/L PLT.

T (°C)	blank V (g/m ² h)	Cl^- V (g/m ² h)	IE_w	Cl^- +PTL V (g/m ² h)	IE_w
20	17.95	6.340	64.7	2.307	87.2
30	43.89	16.84	61.6	8.444	80.8
40	84.59	43.27	48.8	19.36	77.1
50	159.7	88.67	44.5	47.94	70.9

It can be observed that the increase of temperature led to the decrease of IE_w , which means that the adsorption of the inhibitors on steel surface inhibited the corrosion of mild steel in H_3PO_4 solution. With the increase of temperature, the desorption of inhibitor molecules from the steel surface made more steel area exposed to acid solution [47].

The dynamic model can also be used to explain the corrosion inhibition behavior. The apparent activation parameters can be calculated from the Arrhenius equation:

$$\ln V = \frac{-\Delta E_a}{RT} + \ln A \quad (5)$$

where R is the gas constant, E_a is apparent activation energy, A is pre-exponential factor and T is the absolute temperature. Figure 7 shows the Arrhenius plots for mild steel in 7.0 mol/L H_3PO_4 containing Cl^- or Cl^-+PTL .

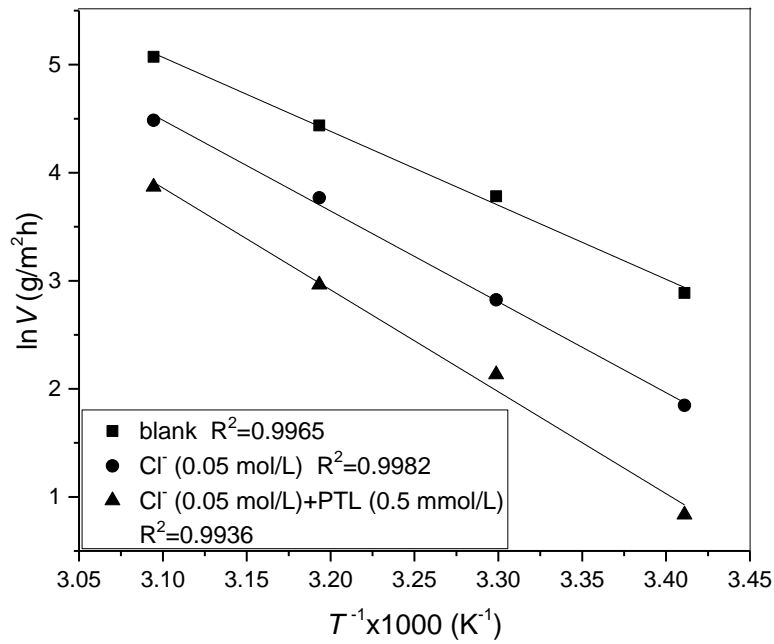


Figure 7. Arrhenius plots of the mild steel in 7.0 mol/L H_3PO_4 .

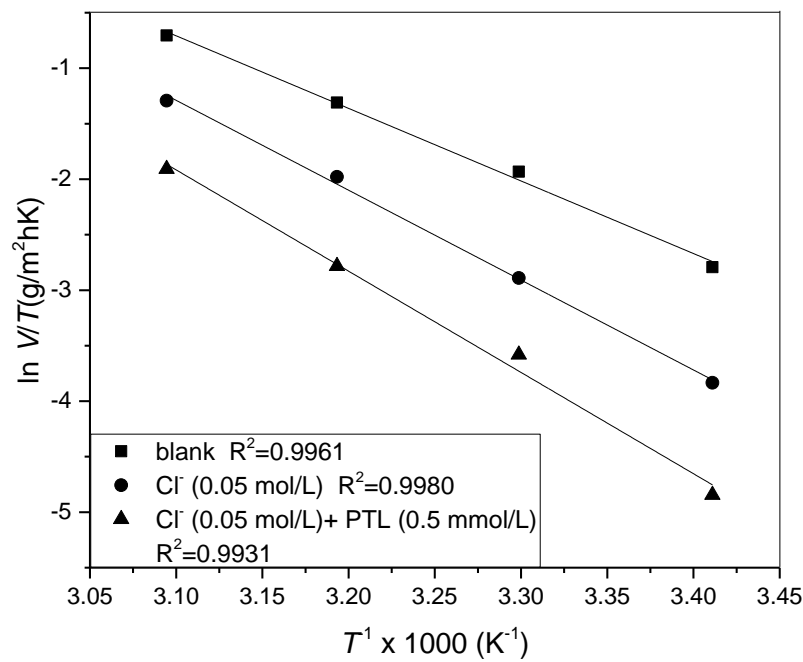


Figure 8. Transition state plots of the mild steel in 7.0 mol/L H_3PO_4 .

The enthalpy of activation (ΔH_a) and entropy of activation (ΔS_a) for the corrosion of mild steel in H_3PO_4 solution can also be calculated by the transition state equation:

$$V = \frac{RT}{Nh} \exp\left(\frac{\Delta S_a}{R}\right) \exp\left(-\frac{\Delta H_a}{RT}\right) \quad (6)$$

where h is Plank's constant and N is Avogadro's number. For ease of calculation, the equation (6) is transformed into the following form:

$$\ln\left(\frac{V}{T}\right) = \left[\ln\left(\frac{R}{Nh}\right) + \frac{\Delta S_a}{R} \right] - \frac{\Delta H_a}{RT} \quad (7)$$

ΔH_a and ΔS_a can be obtained by the slope and intercept of the linear plots, respectively. The plots of $\ln(V/T)$ against $1/T$ for mild steel in 7.0 mol/L H_3PO_4 containing Cl^- or Cl^-+PTL are shown in Figure 8. The values of E_a , ΔH_a and ΔS_a are presented in Table 5.

Table 5. Activation parameters for mild steel in 7.0 mol/L H_3PO_4 in the absence and presence of Cl^- or $Cl^- + PTL$.

Cl^- (mol/L)	PTL (mmol/L)	E_a (kJ/mol)	ΔH_a (kJ/mol)	ΔS_a (J/mol)
0	0	57	54	-35
0.05	0	70	67	0.45
0.05	0.5	78	76	22

The values of E_a , ΔH_a and ΔS_a with the inhibitor is bigger than those without the inhibitor, implying that the corrosion rate of mild steel in 7.0 mol/L H_3PO_4 is mainly decided by the apparent activation energy and the energy barrier of the corrosion reaction rises with addition of the inhibitor. There is a greater energy barrier the combination of Cl^-+PTL than Cl^- alone. The higher values of E_a with the presence of inhibitor can be considered as the physical adsorption mechanism of the inhibitor on the metal surface [48-49]. The positive values of ΔH_a reflect the endothermic property of the steel dissolution process [50]. The negative ΔS_a indicates that the activated complexes represent association rather than the dissociation [51]. In the presence of the Cl^- or Cl^-+PTL , the ΔS_a becomes positive, suggesting that the activated complexes were formed by replacing water molecules with Cl^- and PTL. The increase of entropy is helpful to promote the adsorption of inhibitor molecules on the steel surface [52]

3.5. Adsorption isotherm

The adsorption isotherm is commonly applied to explain the adsorption mechanism of inhibitor molecules on the metal steel. The results show that the experimental data are in good agreement with Langmuir adsorption isotherm:

$$\frac{C}{\theta} = \frac{1}{K_{ads}} + C \quad (8)$$

where C is the concentration of the inhibitor, θ is the degree of surface coverage and K_{ads} is the adsorptive equilibrium constant. The θ was determined by the following formula [53]:

$$\theta = \frac{V_0 - V}{V_0 - V_m} \quad (9)$$

where V_0 is the corrosion rate without inhibitor, V is the corrosion rate with inhibitor and V_m is the smallest corrosion rate.

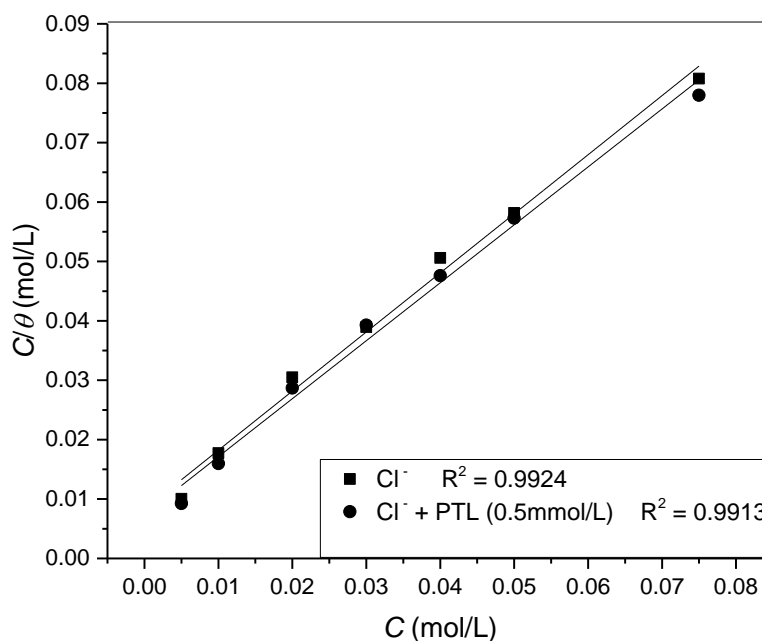


Figure 9. The plots of C/θ against C in 7.0 mol/L H_3PO_4 at 30°C.

Figure 9 shows the dependence of C/θ on the concentration of Cl^- without and with 0.5 mmol/L PTL in 7.0 mol/L H_3PO_4 at 30°C. The regression coefficient values suggest that adsorption of the inhibitors on the surface of mild steel obeys Langmuir adsorption isotherm in 7.0 mmol/L H_3PO_4 . The calculated values of K_{ads} are 1.209×10^2 (mol/kJ) without PTL and 1.355×10^2 (mol/kJ) with PTL, respectively. The larger values of K_{ads} indicate that Cl^- and PTL had a larger trend of adsorption on the surface mild steel in 7.0 mmol/L H_3PO_4 .

The K_{ads} is related to the standard free energy of adsorption (ΔG^0_{ads}) by the formula [54-55]

$$K_{ads} = \frac{1}{55.5} \exp\left(\frac{-\Delta G^0_{ads}}{RT}\right) \quad (10)$$

where 55.5 is the mole concentration of water.

Normally, the ΔG^0_{ads} values equal to or greater than -20 kJ/mol are related to electrostatic interactions (physical adsorption), while equal to or less than -40 kJ/mol are related to chemical adsorption which implies charge sharing or transferring from the inhibitor molecules to the metal surface to form a coordinate bond [56-57]. The obtained values of ΔG^0_{ads} are -22.21 kJ/mol for Cl^-

alone and -22.50 kJ/mol for combination of Cl^- and PTL, respectively. The negative values of $\Delta G_{\text{ads}}^{\circ}$ mean that the adsorption process of Cl^- or PTL was the spontaneous and the magnitude of the values also indicated the coexistence of physical and chemical adsorption, but physical adsorption is absolutely dominant. The results of decrease of inhibition efficiency and $\Delta G_{\text{ads}}^{\circ}$ values with increase of temperature show that the adsorption of Cl^- or PTL on the surface of mild steel in 7.0 mol/L H_3PO_4 is disadvantageous at higher temperature and hence can be regarded as predominantly physical adsorption.

3.6. Synergism effect

The ion pair interaction between anions and organic cations may lead to effect of synergistic inhibition to increase the surface coverage. The synergetic effect can be described by using synergetic parameters which is described as follow [58]:

$$S = \frac{1 - IE_1 - IE_2 + IE_1 \times IE_2}{1 - IE_{1+2}} \quad (11)$$

where IE_1 and IE_2 are the inhibition efficiencies by inhibitor 1 or by inhibitor 2, respectively, and IE_{1+2} is the inhibition efficiency by both inhibitor 1 and inhibitor 2.

Generally, when value of S is < 1 , implying that antagonistic behavior leading to competitive adsorption prevails, whereas $S > 1$ means a synergistic effect. The values of S are given in Table 6. It can be seen that the S values are less than or equal to 1 at the two lowest concentrations of Cl^- , but greater than 1 at most other concentrations of Cl^- , implying that Cl^- and PTL have better synergistic inhibition on mild steel corrosion and effectively promote the improvement of inhibition efficiency in 7.0 mol/L H_3PO_4 .

Table 6. Synergism parameters of Cl^- and 0.5 mmol/L PTL from the three methods for the corrosion inhibition of mild steel in 7.0 mol/L H_3PO_4 at 30°C.

Cl ⁻ (mol/L)	Synergism parameters(S)		
	polarization	EIS	weight loss
0.005	0.82	0.98	0.88
0.01	1.00	1.00	0.96
0.02	1.03	1.10	1.02
0.03	1.11	1.62	1.04
0.04	1.44	1.56	1.33
0.05	1.40	1.38	1.36
0.075	2.59	1.97	2.06
0.1	2.65	1.66	2.57

Steel surface contains positive charge due to $E_{\text{corr}} - E_{q=0}$ (zero charge potential) > 0 in acid solution [59]. Cl^- can be easily adsorbed on the positive charge position of steel surface by electrostatic force. So, zero charge potential becomes less negative, which enhances the adsorption of inhibitors in

cationic form [60]. PTL is easily protonated to form $[\text{PTLH}_x]^{x+}$ in H_3PO_4 . The protonated PTL can be adsorbed to the negatively charged position on the steel surface. There is also a certain degree of interaction between PTL and steel surface through donor-acceptor interactions between the abundance π -electrons, or nitrogen atoms of PTL and the unoccupied d-orbital of the iron. So, chemical and physical adsorption may be acting on the surface of mild steel.

4. CONCLUSION

(1) Cl^- can inhibit the corrosion of mild steel in 7.0 mol/L H_3PO_4 solution to some extent, and the corrosion inhibition increases with the increase of Cl^- concentration. With the addition of 0.5 mmol/L PTL the combination of Cl^- and PTL obviously improves the corrosion inhibition of mild steel. Cl^- and PTL shows better synergistic inhibition effect on mild steel in 7.0 mol/L H_3PO_4 solution by the synergistic parameters,

(2) Potentiodynamic polarization results indicate that Cl^- alone or the combination of Cl^- and PTL acts as a mixed type of inhibitor for mild steel in 7.0 mol/L H_3PO_4 solutions. The corrosion reaction is controlled by charge transfer from EIS

(3) The adsorption of Cl^- on the mild steel surface follows Langmuir adsorption isotherm in the absence or presence of PTL. The values of $\Delta G_{\text{ads}}^{\circ}$ indicate that the adsorption process of inhibitor molecules on the mild steel surface is spontaneous and contains coexistence of physical and chemical adsorption, while physical adsorption is absolutely dominant.

(4) The inhibition efficiencies obtained from potentiodynamic polarization, electrochemical impedance spectroscopy and weight loss studies represent the same trend.

ACKNOWLEDGEMENT:

This work was financially supported by the Innovation and entrepreneurship training fund for College Students of Yunnan University (Grant No.201904028).

References

1. P.B. Mathur and T. Vasudevan, *Corrosion*, 38 (1982) 171.
2. R. Sánchez-Tovar, M.T. Montañés and J. García-Antón, *Corros. Sci.*, 52 (2010) 1508.
3. H. Iken, R. Basseguy, A. Guenbour and A.B. Bachir, *Electrochim. Acta*, 52 (2007) 2580.
4. B. Lin, S. Zheng, J. Liu and Y. Xu, *Int. J. Electrochem. Sci.*, 15 (2020) 2335.
5. Y.J. Yang, H. Liu, D.M. Lu, L. Peng and L. Wang, *Int. J. Electrochem. Sci.*, 14 (2019) 5008.
6. Y.J. Yang, Y.K. Li, L. Wang, H. Liu, D.M. Lu and L. Peng, *Int. J. Electrochem. Sci.*, 14 (2019) 3375.
7. X. Li, S. Deng, X. Xie and G. Du, *Mater. Chem. Phys.*, 181 (2016) 33.
8. R. Najjar, A. M. Abdel-Gaber and R. Awad, *Int. J. Electrochem. Sci.*, 13 (2018) 8723
9. H. Liu, Y.-Ju Yang, L. Wang, S.M. Ma, X.Y. Peng, D.M. Lu, T. Zhao and Z. Wang, *Int. J. Electrochem. Sci.*, 13 (2018) 10718.
10. X. Li, S. Deng, H. Fu and X. Xie, *Corros. Sci.*, 78 (2014) 29.
11. A.M. Al-Bonayan, *Int. J. Electrochem. Sci.*, 10 (2015) 589.

12. X. Li, S. Deng and H. Fu, *Corros. Sci.*, 55 (2012) 280.
13. M. Benabdellah, R. Touzani, A. Dafali, B. Hammouti and S. El Kadiri, *Mater. Lett.* 61 (2007) 1197.
14. L. Tang, X. Li, G. Mu, L. Li and G. Liu, *Appl. Surf. Sci.*, 253 (2006) 2367.
15. T. Poornima, J. Nayak and A.N. Shetty, *Corros. Sci.*, 53 (2001) 3688-3696.
16. L. Wang, *Corros. Sci.*, 48(2006) 608.
17. Y.X. Zhang, Linfei Ji Fuhe Feiliao Gongyixue, Chemical Industry Press. (2008) Beijing, China.
18. D.A. Winkler, *Metals*, 7 (2017) 553.
19. R. Solmaz, G. Kardaş, M. Çulha, B. Yazici and M. Erbil, *Electrochim. Acta*, 53 (2008) 5941.
20. M.M. Saleh, M.G. Mahmouda, Hany M. Abd El-Lateef, *Corros. Sci.*, 154 (2019) 70.
21. H. Rahmani, K.I. Aloui, K.M. Emran, A. El Hallaoui, M. Taleb, S. El Hajji, B. Labriti, E. Ech-chihbi, B. Hammouti, F. El-Hajjaji, *Int. J. Electrochem. Sci.*, 14 (2019) 985.
22. H. Lagaz, S. Zehra, M. R. Albayati, K. Toumiat, Y. El Aoufir, A. Chaouiki, R. Salghi, I.H. Ali, M. I. Khan, I-M. Chung, S. K. Mohamed, *Int. J. Electrochem. Sci.*, 14 (2019) 6667.
23. G. Sigircik, D. Yildirim and T. Tüken, *Corros. Sci.*, 120 (2017) 184
24. G. Žerjav, A. Lanzutti, F. Andreatta, L. Fedrizzi and I. Milošev, *Mater. Corros.*, 68 (2017) 30.
25. M. Mobin, R. Aslam and J. Aslam, *Mater. Chem. Phys.*, 191 (2017) 151.
26. P. Thanapackiam. S. Rameshkumar, S.S. Subramanian and K. Mallaiya, *Mater. Chem. Phys.*, 174 (2016) 129.
27. N. M'hiri, D. Veys-Renaux, E. Rocca, I. Ioannou, N. M. Boudhriouac and M. Ghoul, *Corros. Sci.*, 102 (2016) 55.
28. R Salhi, D.B. Hmamou, E.E. Ebenso, O. Benali, A. Zarrouk and B. Hammouti, *Int. J. Electrochem. Sci.*, 10 (2015) 259.
29. A.Y. Musa, A.B. Mohamad, A.A.H. Kadhum and M.S. Takriff, *Int. J. Electrochem. Sci.*, 11 (2011) 2758.
30. M. Ben Salah, R. Sabot, Ph. Refait, I. Liascukiene, C. Methivier, J. Landoulsi, L. Dhouibi and M. Jeannin, *Corros. Sci.*, 99 (2015) 320.
31. M. Talebian, K. Raeissi, M. Atapour, B.M. Fernández-Pérez, A. Betancor- Abreu, I. Llorente, S. Fajardo, Z. Salarvand, S. Meghdadi, M. Amirasr, R.M. Souto, *Corros. Sci.*, 160 (2019) 108130.
32. S.A. Umoren, O. Ogbobe, I.O. Igwe, E.E Ebenso, *Corros. Sci.*, 50 (2008) 1998.
33. L. Wang, F.C. Yang, J. Ma, Z.W. Fang, S.W. Zhang, Q. Guo, K.L. Lu and Y.X. Wang, *Asian J. Chem.* 25 (2013) 10305.
34. A. Khamis, M.M Saleh, M.I. Awad, *Corros. Sci.*, 66 (2013) 343.
35. X. Li, L. Tang, L. Li, G. Mu and G Liu, *Corros. Sci.*, 48 (2006) 308.
36. N.S. Ayati, S. Khandandel, M. Momeni, M.H. Moayed, A. Davoodi and M. Rahimizadeh, *Mater. Chem. Phys.*, 126 (2011) 873.
37. L. Wang, S.W. Zhang, Q. Guo, H. Zheng, D.M. Lu, L. Peng and J. Xion, *Mater. Corros.*, 66 (2015) 594.
38. A.A. Farag, M.A. Hegazy, *Corros. Sci.*, 74 (2013) 168.
39. A.K. Satapathy, G. Gunasekaran, S.C. Sahoo, K. Amit and P.V. Rodrigues, *Corros. Sci.*, 51 (2009) 2848.
40. K.C. Emeregül, M. Hayvalı, *Corros. Sci.*, 48 (2006) 797.
41. L. Larabi, Y. Harek, M. Traisnel and A. Mansri, *J. Appl. Electrochem.*, 34 (2004) 833.
42. N. Labjar, M. Lebrini, F. Bentiss, N.E. Chihib, S. El Hajjaji and C. Jama, *Mater. Chem. Phys.*, 119 (2010) 330.
43. P. Bommersbach, C. Alemany-Dumont, J.P. Millet and B. Normand, *Electrochim. Acta*, 51 (2006) 4011.
44. M. Lagrenée, B. Mernari, M. Bouanis, M. Traisnel and F. Bentiss, *Corros. Sci.*, 44 (2002) 573.
45. M. Behpour, S.M. Ghoreishi, M. Khayatkashani and N. Soltani, *Corros. Sci.*, 53 (2011) 2489.
46. H. Ashassi-Sorkhabi and M. Eshaghi, *Mater. Chem. Phys.*, 114 (2009) 267.
47. E.E Ebenso and I.B. Obot, *Int. J. Electrochem. Sci.* 5 (2010) 2012.

48. T. Szauer and A. Brand, *Electrochim. Acta*, 26 (1981) 1253.
49. S.M.A. Hosseini, M. Salari, E. Jamalizadeh, S. Khezripoor and M. Seifi, *Mater. Chem. Phys.*, 119 (2010) 100.
50. I.B. Obot and N.O. Obi-Egbedi, *Colloids Surf. A* 330 (2008) 207.
51. A.E. Stoyanova, E.I Sokolova and S.N. Raicheva, *J. Corros. Sci.*, 39 (1997) 1595.
52. M.M Saleh, *Mater. Chem. Phys.*, 98 (2006) 519.
53. I. Sekine, Y. Hirakawa, *Corrosion*, 42 (1986) 272.
54. G. Moretti, F. Guidi and G. Grion, *Corros. Sci.*, 46 (2004) 387.
55. E. Khamis, *Corrosion*, 46 (1990) 476.
56. E. Machnikova, K.H. Whitmire and N. Hackerman, *Electrochim. Acta* 53 (2008) 6024
57. A.K. Singh, and M.A. Quraishi, *Corros. Sci.*, 52 (2010) 1378
58. T. Murakawa, S. Nagaura and N. Hackerman, *Corros. Sci.*, 7 (1967) 79.
59. A. Döner, E.A. Şuhin, G. Kardaş and O. Serindağ, *Corros. Sci.*, 66 (2013) 278.
60. H. Ashassi-Sorkabi, N. Gahlebsaz-Jeddi, F. Hashemzadeh and H.jahani, *Electrochim. Acta*, 51 (2006) 3848.

© 2020 The Authors. Published by ESG (www.electrochemsci.org). This article is an open access article distributed under the terms and conditions of the Creative Commons Attribution license (<http://creativecommons.org/licenses/by/4.0/>).